STUDY ON SIMULATING CALCULATION AND TEST VERIFICATION OF ACCRETED ICE ON TRANSMISSION LINES

J. J. SI, S. C. LIU, L. X. ZHOU, B. LIU, Z. LIU, D.Q. LI and L. LIU

China Electric Power Research Institute, Beijing, P.R.China. Email: sijiajun@hotmail.com

***Abstract*— Relevanting to meteorology, thermodynamic, heat transfer theory and fluid mechanics and being regarded as the process of natural stochastic phase transition, the accreted ice on conductor are dominated by the environmental temperature, wind velocity, water-droplets diameters and conductor structure, etc. So as to study the influence rules of these factors and to achieve the real effect of accreted ice in this paper, the algorithm module of the perpendicular collision process of super-cooled water droplets with the conductor has been developed and the simulation studies on accreted ice under different conditions have been carried out on the basis of theoretical researches. Then some experiments are taken in the phytotron to verify the feasibility of the calculation algorithm.**

***Keywords*— Transmission Lines; Ice Accretion; Ice Intensity; Local Collision Efficiency (LCE); Numerical Simulation;**

I. INTRODUCTION

The growth of accreted ice on conductor is a kind of physical phenomenon that super-cooled water droplets release the latent heat on the surface of the cable. This process of natural stochastic phase transition is dominated by local meteorological, topographical conditions and surface conditions of the conductor.

The hazards of accreted ice on transmission lines expands increasingly and becomes more and more severe these years with the frequent occurrence of global extreme climate (Li *et al.*, 2006). On considering the complexity and inter-disciplinarily of this problem, studies on accreted ice on conductor have a great significance for resisting the ice disaster of power system and improving the safe and stable operation of the grids (Zhang and Chen, 2004).

The most important problems of the ice accretion model on conductor are the calculation of the complex shape model in the flow field under high Reynolds numbers and the simulation of the water-droplet impingement characteristics. In this article, a program of ice accretion has been developed to solve these problems and some experiments have then been taken in artificial climate chamber to verify the feasibility of the calculation algorithm.

II. SIMULATING CALCULATION MODEL

The accreted ice on conductor phenomena is considered as a process of perpendicular collision in the radial direction of super-cooled water droplets with the conductor under the airflow effect. The flow field calculation is the key module for the model (Bazeos and Beskos, 1990). Water droplet collision trajectory calculation is firstly simulated for obtaining LCE and the movement simulation of water film on the conductor surface is carried out for the ice increment distribution in solving heat balance equation (Lozowski *et al.*, 1983). The local heat transfer coefficient is then evaluated through airflow velocity distribution at the external edge of boundary layer which will be used to calculate freezing coefficient of super-cooled water droplets in each unit in the following thermodynamic analysis (Fu *et al.*, 2006). At last, according to the ice accretion volume obtained and the virtue boundary moving technology, a new ice accretion surface can be obtained and a new ice accretion structure will be reconstructed.

A. Flow Field Calculation

Water droplets movement in air flow refers to the gas-liquid two-phase characteristics (Guo *et al.*, 2011a).

Division of Mesh Partition of Calculation Region

In the model adopted, structural mesh was used in the external part of ice accretion region. On the surface closely sticking to the conductor, local refined O-type meshes were used in the boundary layer region, and dynamic mesh technology was adopted in the freezing region.

Governing Equations

Based on two dimensional Navier-Stocks governing equations and Reynold averaging technology, the governing equations are then obtained by mass conservation equation.

$$\frac{\partial(\rho u)}{\partial x}+\frac{\partial(\rho v)}{\partial y}=0, \qquad (1)$$

$$\begin{aligned}\frac{\partial(\rho uu)}{\partial x}+\frac{\partial(\rho vu)}{\partial y}=-\frac{\partial p}{\partial x}+\frac{\partial}{\partial x}\left(\mu\frac{\partial u}{\partial x}\right)\\+\frac{\partial}{\partial y}\left(\mu\frac{\partial u}{\partial y}\right)+\frac{\partial}{\partial x}\left(-\rho\overline{u'u'}\right)+\frac{\partial}{\partial y}\left(-\rho\overline{u'v'}\right)\end{aligned}, \qquad (2)$$

$$\begin{aligned}\frac{\partial(\rho uv)}{\partial x}+\frac{\partial(\rho vv)}{\partial y}=-\frac{\partial p}{\partial y}+\frac{\partial}{\partial x}\left(\mu\frac{\partial v}{\partial x}\right)\\+\frac{\partial}{\partial y}\left(\mu\frac{\partial v}{\partial y}\right)+\frac{\partial}{\partial x}\left(-\rho\overline{u'v'}\right)+\frac{\partial}{\partial y}\left(-\rho\overline{v'v'}\right)\end{aligned}, \qquad (3)$$

In the formulas, ρ represents air density (kg·m^{-3}), u and v refer to velocity components of flow field along the directions of x-axis and y-axis respectively (m/s), p represents the pressure (Pa), μ represents the dynamic viscosity (kg·m^{-1}·s^{-1}), $-\rho\overline{u'u'}$, $-\rho\overline{u'v'}$, $-\rho\overline{v'v'}$ represent Reynolds stress. According to the calculation pneumatic characteristics of trailing vortex of circular detouring flow, the turbulence model adopts the $k-\omega$ model (Guo *et al.*, 2011b; Wright, 1993).

Algorithm and Boundary Conditions

In the algorithm, the momentum equation and the pressure correction equation are adopted to solve the pressure coupling equations. The boundary conditions are as follows: (1) Inflow boundary conditions: velocity inlet where the pressure adopts two-order extrapolation; (2) Outflow boundary conditions: $\partial\Phi/\partial\mathbf{n}=0$; (3) No slip wall boundary conditions: u=0, v=0, $\partial P/\partial\mathbf{n}=0$ and k and ε are treated as wall function (Makkonen, 2000).

B. Calculation of Water Droplet Collision Trajectory

Calculation of Water Droplets Trajectory

The discrete-time motion trajectory equations are implemented by Messinger (1953) as:

$$\frac{dw_x}{dt}=\frac{C_D Re}{24}\times\frac{1}{K}(u-w_x)\,, \quad (4)$$

$$\frac{dw_y}{dt}=\frac{C_D Re}{24}\times\frac{1}{K}(v-w_y)\,, \quad (5)$$

where

$$K=\frac{2r^2\rho_w V_0}{9\mu D}\,, \quad (6)$$

In the formula, K refers to inertial parameter of water droplets, Re refers to Reynolds number of relative movement, w_x and w_y refer to velocity of water droplets in x and y direction (m/s), r refers to radius of water droplets (mm), D refers to diameter of conductor (mm), V_0 refers to velocity of incoming flow (m/s), ρ_w refers to water density (kg·m^{-3}), and C_D refers to drag force coefficient (Messinger, 1953).

Calculation of Collision Efficiency

The general collision efficiency (GCE) reflects the inertial accumulation efficiency of water droplets. The shape of ice formed along the object can be deduced after determining the amount distribution of collision water along the object surface. For the discrete-time distribution research of water amount along the object surface, it is required to calculate the local water collection capability of the infinitesimal surface. The perpendicular collision of super-cooled water droplets with the conductor at speed of w_x=u and w_y=v=0 have been programmed on the basis of discrete-time model by virtue of UDF function. Whereas, on considering the random position between two water-droplets, it is necessary to interpolate the fed back positions of water droplets into mesh nodes, and the LCE and the positions of local collision of super-cooled water droplets can then be obtained through discrete-phase model, shown in Fig.1.

LCE can be defined as follows:

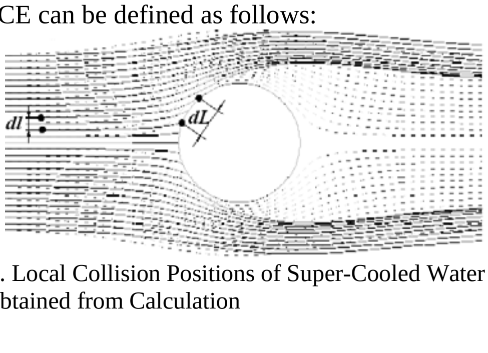

Fig. 1. Local Collision Positions of Super-Cooled Water Droplets Obtained from Calculation

$$\beta=\frac{dl}{dL}\,, \quad (7)$$

In which, dl refers to the difference of original longitudinal coordinates of upper and lower water-droplets trajectories on the infinitesimal surface, dL refers to the surface length between upper and lower boundaries on the infinitesimal surface (Makkonen, 2000).

C. Calculation of Ice Accretion

Calculation of Surface Water Film Motion

Under the condition of high Reynolds number, the water film on the cylindrical surface can be divided into two streams of water flow moving toward different directions from the separation point. The forces which influence the movement directions of water film refer to air resistance and gravity. Two forces can be represented as follows.

$$V_t=\frac{\tau_{air}}{\mu}\frac{d}{2}\,, \quad (8)$$

$$V_g=\frac{1}{3}\frac{\gamma}{\mu}d^2\sin\theta\,, \quad (9)$$

If $V_t > V_g$, the water film will move upward, conversely, the water film will move downward. Assuming that the motion direction of the film is from element i to element i+1 and neglecting the water falling influence, the total quantity of water-droplets accumulated is the summation of the mass of droplets collided m_i and unfrozen droplets m_r of anterior time-step. The film average velocity can be deduced as follows (Gent, 1990).

$$q=\frac{1}{3}\frac{\gamma}{\mu}d^3\sin\theta-\frac{\tau_{air}d^2}{2\mu}\,, \quad (10)$$

The water film velocity can then be estimated as below:

$$V=\frac{q}{d}=\frac{1}{3}\frac{\gamma}{\mu}d^2\sin\theta-\frac{\tau_{air}d}{2\mu}\,, \quad (11)$$

In which, d refers to the film thickness. As a result, the formula for film thickness and average velocity in different motion direction can be deduced (Yang, 2012).

Calculation of Surface Heat Balance

With regard to heat flux items, such as Joule heat flow generated by transmission current, scholars proposed the heat balance equation of ice accretion shown in formula (12) after multiple times of correction (Personner and Gayet, 1988).

$$\begin{aligned}&q_f+q_v+q_k+q_a+q_n+q_R=\\&q_c+q_e+q_l+q_s+q_i+q_r+q_q\end{aligned}\,, \quad (12)$$

where, q_f refers to latent heat released on freezing, q_v refers to heat generated by air friction to water droplets on the ice surface, q_k refers to kinetic energy heat generated by collision of super-cooled water-droplets with ice surface, q_a refers to heat released during the process of cooling the ice from T_f to stable temperature T_s on the ice accretion surface, q_n refers to sunlight short-wave radiation heat, q_R refers to Joule heat flow generated by transmission current, q_c refers to convective thermal losses from ice surface and air, q_e refers to heat losses of evaporation and sublimation of the ice surface, q_l refers to heat absorbed as the temperature of super-cooled water droplets which collide with the conductor rises to T_f, q_s refers to heat losses generated by long wave radiation of the ice surface, q_i refers to heat conduction loss, q_r refers to heat losses generated by water-droplets detach from ice surface, q_q refers to thermal losses generated by air forced convection.

Calculation of Ice Density

Related to influence factors on accreted ice as well as dynamic heat balance process of ice surface, the Macklin parameter model was selected for the calculation in this paper.

$$\rho_i = 0.218 R_d^{0.51} \qquad R_d \le 10\,, \tag{13}$$

$$\rho_i = R_d (1.13 R_d + 2.15)^{-1} \quad 10 < R_d \le 60\,, \tag{14}$$

$$\rho_i = 0.84 \qquad R_d > 60\,, \tag{15}$$

where R_d=-rV / T , r is radius of water-droplets, V is wind speed, T is ice surface temperature.

III. RESULT AND ANALYSIS

A. Influence of Air Temperature

When the glaze forms, the temperature is relatively high, ranging from -5ºC to 0ºC, while for the soft rime, the temperature ranges from -15ºC to -10ºC. And the temperature of hard rime is generally between glaze and soft rime, ranging from -9ºC to -3ºC. Normally the temperature range which easily leads to ice accretion is from -6ºC to 0ºC. In this article, six temperature conditions: -15ºC, -10 ºC, -7 ºC, -5 ºC, -3ºC, -2ºC have been chosen for the accreted ice simulation. Other calculation parameters are shown in Table 1.

Ice Intensity

The calculation results shown in Fig. 2 can be found that both the ice intensity and the ice thickness at stagnation point increase with the duration. The change of LCE on the ice surface is not obvious. But it is clear that the ice intensity increases with the ambient temperature, while the ice thickness at stagnation point decreases with the temperature because the ice accretion on the conductor surface transforms gradually from soft rime to glaze with the ice temperature and ambient temperature. The higher the ice temperature is, the smaller the ice volume will be. These conclusions are in concert with the actual situation and prove the exactness of numerical simulation.

Collision Efficiency

Representing the relationship between the GCE on the ice surface of conductor and duration under different ambient temperature conditions, the collision efficiency reduces gradually with the duration when the temperature ranges from -15ºC to -5ºC, shown in Fig. 3. As the ice accumulation causes the modification of flow effect and the reduction of windward area, the cylindrical section will become streamlined body gradually and then more water droplets will flow in the detouring way. This makes the water droplet collection coefficient reduce.

Table 1. Other Calculation Parameters

Conductor diameter	21.6 mm
Wind velocity	5 m/s
Diameter of water droplet	25 μm
Liquid-water content	0.6 g/m^3

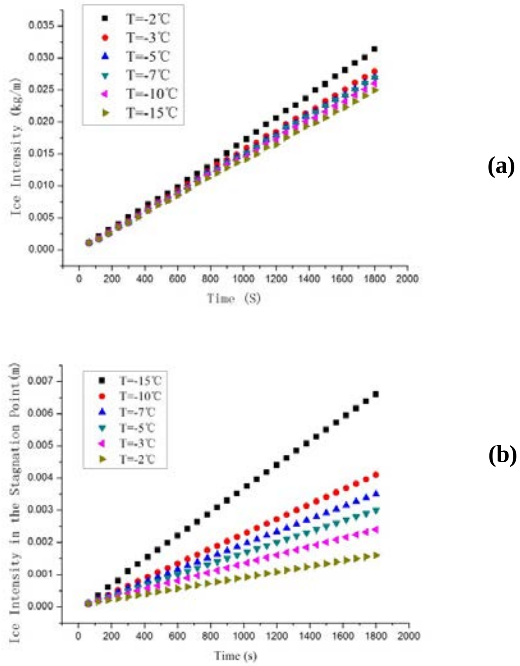

Fig. 2. Calculation Result (a) Relation between Ice Intensity and Duration, (b) Relation between Ice Accretion Thickness and Duration at the Stagnation Point

When the temperature is -3ºC, the collision efficiency will decrease firstly, and then it grows gradually 10 minutes later. It shows that, at -3ºC the increasing of soft rime occurs, i.e. the accumulation process is wet growth at stagnation point. Meanwhile, the water-droplets start to flow along cylindrical circumference and ice shape increases uniformly along cylindrical circumference. However, the position far away from the stagnation point, the ice accretion still refers to dry increasing process. In a relatively short period, the accretion process is similar to the dry growth in low-temperature, and the LCE decreases with the increase of ice thickness. Through a period of energy transfer on the ice surface, the homogeneous growth of ice shape in circumferential direction makes both windward section and general collision efficiency increase.

At -2ºC, the ice accretion on the conductor surface shows the wet growth process and the ice shape will increase uniformly along cylindrical circumference, i.e. the diameter of cylinder as well as GCE will increase gradually. The ice shape is as shown in Fig. 4.

B. Influence of Wind Velocity

Normally, the faster the wind blows, the thicker the ice forms on conductor. Wind direction will influence the shape of ice accretion. When the wind direction is perpendicular to the conductor, the ice will form on the windward face firstly and then the eccentric ice shape forms; when the wind direction is parallel to the con-

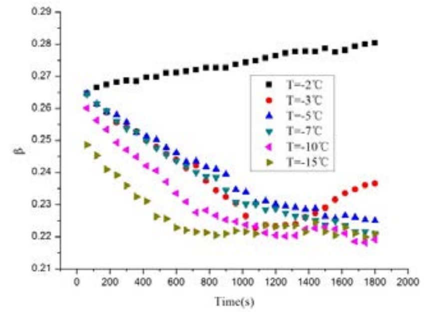

Fig. 3. Relation between GCE of Water Droplets and Duration at Different Temperature

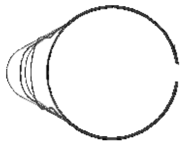

Fig. 4. Ice Shape on Conductor Surface (Corresponding Temperature for Ice Shape Contour from External to Internal are respectively -15, -10, -7, -3ºC)

Table 2. Other Calculation Parameters

Air temperature (℃)	-15	-12	-2
Conductor diameter (mm)		21.6	
Liquid-Water Content (g/m^3)	0.3	0.3	0.6

ductor, ice accretion will form uniformly. In this study, three different temperature: -15ºC, -12ºC, -2ºC and six different wind speed: 3m/s, 5m/s, 6 (or 8) m/s, 10m/s, 15m/s, 20m/s have been taken into account in the influence rules calculation. Other calculation parameters are shown in Table 2.

Ice Intensity

The variation curves of ice intensity with the wind velocity in Fig. 5 show that ice intensity increases linearly with the duration and the wind speed. For the higher the wind velocity is, the higher the inertial parameter K and the LCE will be, which leads to the increase of ice intensity. When the wind velocity increases, the collision efficiency on the conductor will grow, thickening the ice accretion and accelerating the water droplets speed. Meanwhile, the increased collision kinetic energy of water droplets and the friction heating energy of water droplets raise the temperature of ice surface and droplets make the freezing coefficient reduce correspondingly.

Collision Efficiency

Figure 6 shows the relationship between the GCE of water-droplets on ice surface and duration under different wind velocity conditions at -15ºC. The collision efficiency reduces gradually with the duration when the wind speed ranges from 3m/s to 20m/s. When the wind speed is relatively slow, the ice accretion amount and the GCE is relatively small, the LCE shows a slight increasing process. Alternatively, when the wind velocity is relatively high and the GCE and LCE are relatively large, the ice shape will form a streamlined body and the collision efficiency will reduce with time.

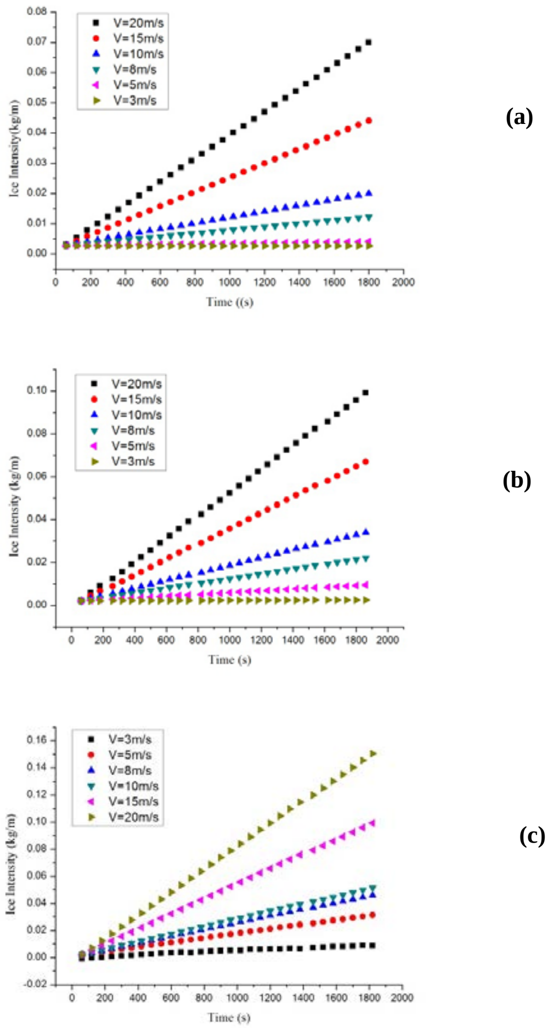

Fig. 5. Calculation Result. Relation between Ice Intensity and Duration at: (a) -15ºC, (b) -12ºC, (c) -2ºC

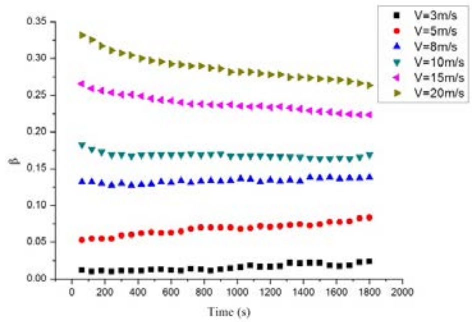

Fig. 6. Relation between GCE and duration

The ice shape under different wind velocity conditions at -15ºC is shown in Fig. 7. It can be seen that the collision efficiency of water droplets at stagnation point is the largest and the value decreases gradually along the circumferential direction. It is because that the influence of flow field around the stagnation point is minimum, where the deviation of water droplets away from streamline is relatively large and the water collection efficiency is relatively large. In addition, with the in-

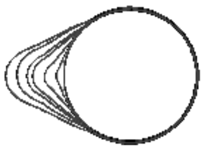

Fig. 7. Ice Shape on Conductor Surface at -15ºC (Corresponding Wind Velocity for Ice Shape Contour from External to Internal are respectively 3m/s, 5m/s, 8m/s, 10m/s, 15m/s, 20m/s)

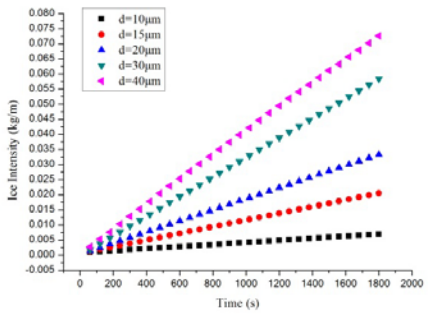

Fig. 8. Relation between Ice Intensity and Duration at -15ºC

Table 3. Other Calculation Parameters

Air temperature (ºC)	-15
Conductor diameter (mm)	21.6
Wind velocity (m/s)	10
Liquid-water content (g/m^3)	0.3

creaseing of wind speed, both the collision area and the general collision efficiency will increase.

C. Influence of Water Droplet Diameter

In case of glaze, the diameter of super-cooled water droplets is relatively large, ranging from 10μm to 40μm, and the medium-volume water droplets diameter is about 25μm; while the diameter of water droplets ranges from 1μm to 20μm in case of soft rime, and the medium-volume water droplets diameter is about 10μm. For hard rime, the diameter of water droplets ranges from 5μm to 35μm, and the medium-volume water droplet diameter is about 15μm-18μm. In this paper, five droplets diameters: 10μm, 15μm, 20μm, 30μm, 40μm have been chosen for the simulation and other parameters are shown in Table.3.

Ice Intensity

The variation curves of ice intensity with the duration under different super-cooled water droplet diameters are shown in Fig. 8, proving that the freezing amount increases linearly. According to the change curves of freezing amount under different super-cooled water droplets, it can be known that with the increase of super-cooled water droplets diameters, the freezing amount will increase constantly due to the relative inertia and LCE. As a result, most droplets collide with the conductor surface while only a small amount detour the conductor.

Collision Efficiency

Figure 9 refers to the contour of ice shape of different super-cooled water droplet. The influence of the flow field around the stagnation point becomes lesser which resulted in a relatively large deviation between water droplets and stream lines. As a result, the collection coefficient, the collision scope as well as the GCE become large with the increase of water droplet diameter. In addition, the collision efficiency of water droplets is the maximum at the stagnation point and it reduces gradually along circumference.

IV. ICE ACCRETION TEST

A. Test Device

(1) Test conductor:

The test conductor is JL/G1A-240/30 whose diameter is 21.6mm.

(2) Climate-Control Chamber:

The test is conducted in phytotron whose diameter is 5.2m and height is 9m, meeting the test requirements.

(3) Spraying and wind velocity adjustment system:

The rain fall nozzles distributed around the conductor in the phytotron is sprayed by the high-pressure water pump with the water mist droplets diameters ranging from 5μm to 500μm. The air-blast system in the laboratory is realized through a 5×7 array of blasts.

The wind velocity and direction of each outlet in the array can be adjusted for realizing different accreted ice conditions; as a result, the wind velocity nearby the conductor can be controlled within 0m/s-8m/s.

B. Test Result

After arranging the test samples and closing the artificial climate chamber door, the refrigerator began to work. Then the weighing instrument should be reset and the spray pump should be launched when the conductor temperature decreased to the test value. The ice thickness was recorded every 10min until the end of the experiment.

In this paper, three influence factors of accreted ice on conductor mentioned above have been verified by experiments, among which the temperature is -3ºC, the wind velocity is 20m/s and the water droplet diameter is 30μm. The result is shown in Fig. 11 and Table 5. Due to the simulation results, the ice intensity is respectively 0.29kg/m at -3ºC, 1.06kg/m when the wind speed is 20m/s and 0.53kg/m when the droplets diameter is 30μm after 300 minutes, showing that the simulation calculation results of ice intensity are consistent with test data. The results prove that the model is correct and effective.

V. CONCLUSIONS

Through the comparison between calculation result and test data, the following conclusions can be obtained.

(1) The ice intensity under different working conditions is different due to the difference of collision effi-

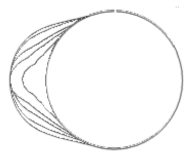

Fig. 9. Ice Shape on Conductor Surface at -15ºC (Corresponding Water Droplet Diameters for Ice Shape Contour from External to Internal are respectively 10μm, 15μm, 20μm, 30μm and 40μm)

Fig. 10. Conductor Arrangement and Test Result

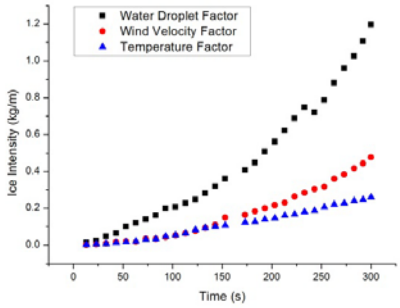

Fig. 11. Experiments Results

Table 5. Comparison of Calculation and Experiments

Calculated Time (min)	Influencing Factor	Average Test Value (kg/m)	Calculated Value (kg/m)
300	Temperature	0.26	0.29
	Wind speed	1.20	1.06
	Water droplet diameter	0.48	0.53

ciency. The ice shape is mainly determined by LCE and ambient temperature, while the ice intensity is determined by GCE.

(2) Within a certain ambient temperature scope, the ice intensity on the conductor surface increases with the temperature; however, the maximum ice thickness reduces with the constant rising of temperature.

(3) The ice intensity on the conductor surface increases while the freezing coefficient reduces with the wind velocity. Two kinds of mutual opposed influence factors determine that there exists a critical wind velocity which is the most suitable for ice accretion.

(4) The ice shape modifies gradually from bluff body to streamlined body during the dry increasing process. Under the wet increasing process, the local curvature radius of ice shape in the windward region will increase, and the ice densities on all conductors' surface are almost consistent with each other.

(5) From the experimental studies' results in artificial climate room, the solution of numerical model agrees favorably with experimental result, proving that the algorithm model can be adopted for the effect prediction of accreted ice on conductor.

ACKNOWLEDGMENT

The authors are grateful for financial support from the National Natural Science Foundation of China (51678548) and the Science and Technology Project of the State Grid (GC71-14-006).

REFERENCES

Bazeos, N. and D.E. Beskos, *Numerical Determination of Wind Pressure on 2-D Structures (1st ed)*, Computational Mechanics Publications, Germany (1990).

Fu, P., M. Farzaneh and G. Bouchard, "Two Dimensional Modeling of the Ice Accretion Process on Transmission Line Wires and Conductors," *J. Cold Regions Science and Technology*, 46, 132-146 (2006).

Gent, R.W., *TRAJICE2-A Combined Water Droplet Trajectory and Ice Accretion Prediction Program for Aerofoil*, R. DRA Technical Research Project (1990).

Guo, H., P.-Q. Liu, Q.-L. Qu, S.-C. Liu, J.-C. Wang and Y.-X. Di, "Two Dimensional Numerical Simulation of the Rime Accretion Process on Transmission Lines," *J. Engineering Mechanics*, 28, 212-218 (2011a).

Guo, H., P.-Q. Liu, Q.-L. Qu and Z.-Z. Duan, "Estimation Engineering Method of Rime Accretion Process on Transmission Lines," *J. High Voltage Engineering*, 37, 1041-1049 (2011b).

Li, Z.-M., Z.-P. Yu and Y.-F. Hu, "Transmission Line Regelation Harm and Protection," *J. Insulators and Surge Arresters*, **21**, 12-14 (2006).

Lozowski, E.P., J.R. Stallabrass and P.F. Hearty, "The Icing of an Unheated, Non-rotating Cylinder, Part I: A Simulation Model," *J. Journal of Climate and Applied Meteorology*, **22**, 2053-2062 (1983).

Makkonen, L., "Models for the growth of rime, glaze, icicles and wet snow on structures," *J. Phil. Trans. R. Soc. Lond A*, **358**, 2913-2939 (2000).

Messinger, B.L., "Equilibrium temperature of an unheated icing surface as a function of airspeed," *Journal of the Aeronautical Sciences*, **20**, 195-200 (1953).

Personner, P. and J.F. Gayet, "Ice Accretion on Wires and Anti-Icing Induced by Joule Effect," *J. Journal of Applied Meteorology*, **27**, 101-104 (1988).

Wright, W.B., "Advancement in the LEWICE Ice Accretion Model," *J. AIAA Paper*, **93**, 171-188 (1993).

Zhang, D.-L. and W.-J. Chen "Numerical Simulation of the Rime Ice Accretion Process on Airfoil," *J. Journal of Aerospace Power*, **19**, 137-141 (2004).

Yang, X., *Research on Ice Accretion and Ice-melting Calculation of Overhead Transmission Lines*, aster's Thesis of North China Electric Power University. Beijing. China (2012).

Received: November 28, 2016.
Sent to Subject Editor: December 15, 2016.
Accepted: June 12, 2017.
Recommended by Subject Editor: Gianfranco Caruso